

**AAS 12-017**

## Design of Spacecraft Missions to Remove Multiple Orbital Debris Objects

Brent W. Barbee\*, Salvatore Alfano<sup>†</sup>, Elfego Piñon<sup>‡</sup>, Kenn Gold<sup>‡</sup>, and David Gaylor<sup>‡</sup>

\*NASA-GSFC, <sup>†</sup>CSSI, <sup>‡</sup>Emergent Space Technologies, Inc.

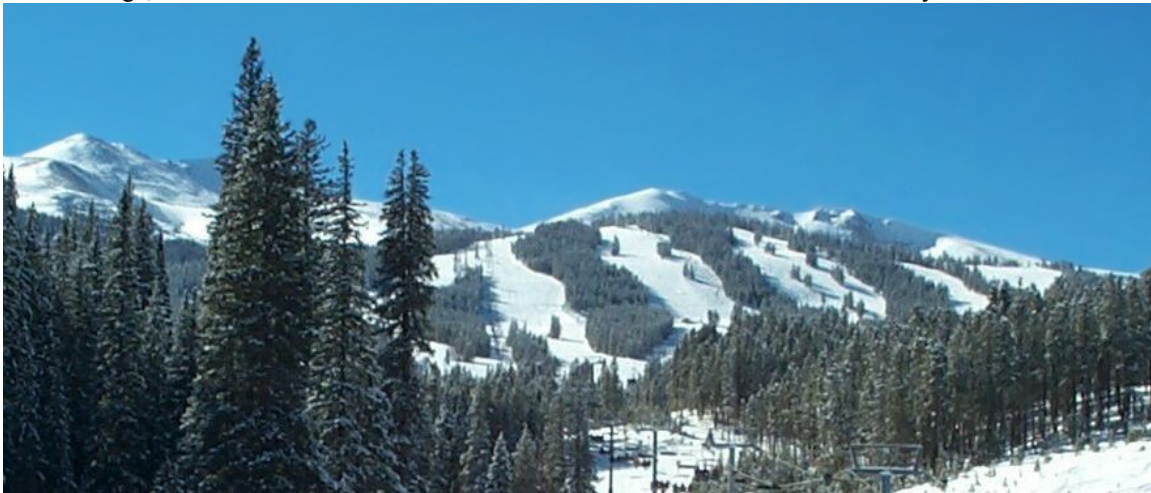
---

### 35<sup>th</sup> ANNUAL AAS GUIDANCE AND CONTROL CONFERENCE

---

February 3 - February 8, 2012  
Breckenridge, Colorado

Sponsored by  
Rocky Mountain Section



AAS Publications Office, P.O. Box 28130 - San Diego, California 92198

## DESIGN OF SPACECRAFT MISSIONS TO REMOVE MULTIPLE ORBITAL DEBRIS OBJECTS

**Brent W. Barbee<sup>\*</sup>, Salvatore Alfano<sup>†</sup>, Elfego Piñon<sup>‡</sup>,  
Kenn Gold<sup>§</sup>, and David Gaylor<sup>¶</sup>**

The amount of hazardous debris in Earth orbit has been increasing, posing an ever-greater danger to space assets and human missions. In January of 2007, a Chinese ASAT test produced approximately 2600 pieces of orbital debris. In February of 2009, Iridium 33 collided with an inactive Russian satellite, yielding approximately 1300 pieces of debris. These recent disastrous events and the sheer size of the Earth orbiting population make clear the necessity of removing orbital debris. In fact, experts from both NASA and ESA have stated that 10 to 20 pieces of orbital debris need to be removed per year to stabilize the orbital debris environment. However, no spacecraft trajectories have yet been designed for removing multiple debris objects and the size of the debris population makes the design of such trajectories a daunting task. Designing an efficient spacecraft trajectory to rendezvous with each of a large number of orbital debris pieces is akin to the famous Traveling Salesman problem, an NP-complete combinatorial optimization problem in which a number of cities are to be visited in turn. The goal is to choose the order in which the cities are visited so as to minimize the total path distance traveled. In the case of orbital debris, the pieces of debris to be visited must be selected and ordered such that spacecraft propellant consumption is minimized or at least kept low enough to be feasible. Emergent Space Technologies, Inc. has developed specialized algorithms for designing efficient tour missions for near-Earth asteroids that may be applied to the design of efficient spacecraft missions capable of visiting large numbers of orbital debris pieces. The first step is to identify a list of high priority debris targets using the Analytical Graphics, Inc. SOCRATES website and then obtain their state information from Celestrak. The tour trajectory design algorithms will then be used to determine the itinerary of objects and  $\Delta v$  requirements. These results will shed light on how many debris pieces can be visited for various amounts of propellant, which launch vehicles can accommodate such missions, and how much margin is available for debris removal system payloads.

### INTRODUCTION

Emergent Space Technologies, Inc. has developed specialized algorithms to design trajectories for rendezvous with multiple near-Earth asteroids (NEAs). These algorithms were originally developed for the 4<sup>th</sup> annual Global Trajectory Optimization Competition (GTOC4), held during 2009, in which the problem posed was to maximize the number of asteroids that could be intercepted during

<sup>\*</sup> Aerospace Engineer, NASA GSFC, Code 595, 8800 Greenbelt Road, Greenbelt, MD 20771, USA.

<sup>†</sup> Senior Research Astrodynamist, Center for Space Standards and Innovation (CSSI), 7150 Campus Drive, Suite 260, Colorado Springs, CO, 80920.

<sup>‡</sup> Senior GN&C Engineer, Emergent Space Technologies, Inc., 6411 Ivy Lane, Suite 303, Greenbelt, MD 20770.

<sup>§</sup> Director of R&D, Emergent Space Technologies, Inc., 6411 Ivy Lane, Suite 303, Greenbelt, MD 20770.

<sup>¶</sup> Vice President, Emergent Space Technologies, Inc., 6411 Ivy Lane, Suite 303, Greenbelt, MD 20770.

the course of a single mission using a particular set of spacecraft propulsion and launch parameters. Those algorithms are also applicable to the problem of rendezvous with multiple pieces of orbital debris for the purpose of active orbital debris mitigation. For debris mitigation, a propellant-efficient approach is required in which one object is targeted initially and from that first orbit subsequent objects are targeted for removal. The technology developed for asteroid mission design has therefore been modified to perform trajectory and mission design for a spacecraft that would participate in active debris removal efforts.

### The Current State of the Orbital Debris Problem

Significant growth of the orbital debris environment began with the June 1961 explosion of a human-made vehicle which created more than 300 trackable objects. Over the ensuing 45 years, the number of large debris objects (> 10 cm in size) grew by about 300 per year.<sup>1</sup> The primary source of orbital debris in Low Earth Orbit (LEO) is the fragmentation of space vehicles, though the problem continues to worsen through the accumulation of launch vehicle orbital stages and derelict spacecraft, as shown in Figure 1 (note that some debris from the major breakups of 2007 and 2009 have yet to be officially cataloged). At least 190 spacecraft are known to have been involved in fragmenting breakups, and at least 50 more have been involved in lower-level anomalous fragmentation events.<sup>2</sup> While orbital debris smaller than 10 cm can collide with operational satellites and render them inoperative due to hypervelocity impacts, it is generally believed that debris larger than 10 cm presents the possibility of destroying another satellite and causing a large fragmentation event. Although the risk is currently low, with only a single confirmed loss of a functioning satellite (Iridium-33) due to human-made orbital debris, the problem is expected to worsen, and a significant risk is thus presented to the nearly 1000 operational satellites in LEO.

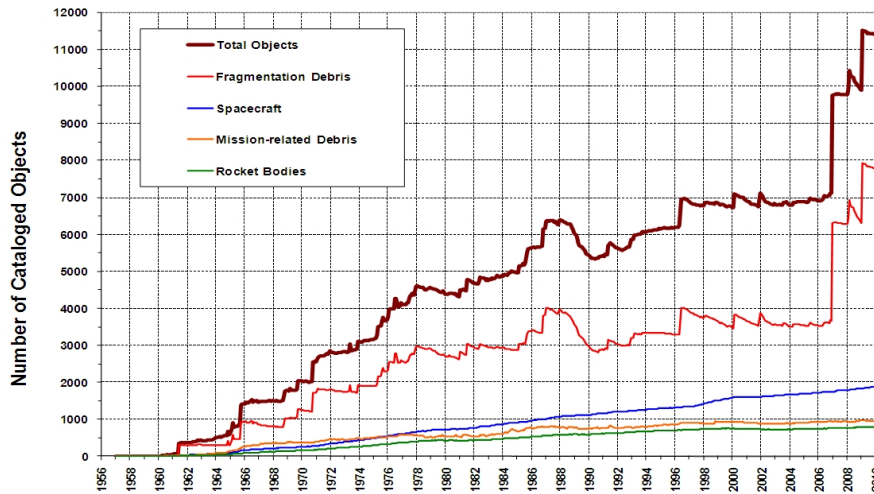


Figure 1. Growth of the Cataloged Satellite Population (From Ref. 2)

The catalog of the US Space Surveillance Network currently lists approximately 15000 trackable objects, accounting for approximately 5800 tons of on-orbit mass. The total population is thought to exceed 20000 objects larger than 10 cm (Ref. 1). The first position paper from the International

Academy of Astronautics (IAA) in 1993 (updated in 2001)\* states that "... all investigations addressing the long-term evolution of orbital debris conclude that without changes to the way space missions are performed, regions of near-Earth space will become so cluttered by debris that routine operations will not be possible." Over the 15 years that followed, the adoption of international orbit debris mitigation guidelines reduced the rate of growth of new orbital debris. The updated IAA position paper states "Remediation of the near-Earth space environment was still seen as a principal long-term objective, but technology and/or cost considerations hampered the development and deployment of proposed debris removal techniques."

The environment in Geosynchronous Orbit (GEO) is also becoming congested, with some 520 known space objects accounting for more than 1200 tons of on-orbit mass. Orbital debris in GEO is the product of two known fragmentation events with evidence of perhaps as many as ten separate events. Much of the debris at both LEO and GEO is concentrated in orbital bins of objects within 50 km altitude and 2° inclination of each other. A particular debris band in LEO contains 800 objects with a total mass of 300 tons, and a similar group exists at GEO where a particular bin contains 240 objects with a total mass of 790 tons.<sup>3</sup> These specific regions have critical mass concentrations which are predicted to trigger cascading fragmentation events in the coming decades.

### **The Chinese ASAT Test and the Iridium Collision**

Two recent events have caused particularly large increases in the known orbital debris environments. In January of 2007, the Chinese government conducted an anti-satellite (ASAT) test in which the FengYun 1C satellite was destroyed. This single event resulted in more than 2900 pieces of orbital debris greater than 10 cm in size, many of which are not yet included in the debris catalog.<sup>3</sup> The first unintentional collision of two satellites occurred in February of 2009 when the operational Iridium-33 satellite collided with the inoperative Cosmos 2251. This accident generated more than 1600 pieces of large debris in two separate clouds. These events taken together represent an increase in the collision risk for operational satellites in orbits between 750 and 900 km altitude.<sup>4</sup> The sheer magnitude of these events and the size of the collision fragment clouds demonstrate the necessity of preventing future collisions.

### **Estimates of Cascading Failure for LEO**

Predictions generated by NASA of the orbital debris environment show that even an immediate halt of all launch activities will still result in an increase in collision events, and thus an increase in the debris environment. The projected mass of collision fragments greater than 10 cm is expected to first exceed those due to end of life explosions or fragmentation events by the year 2040, and to exceed it by a factor of two by the year 2100.<sup>5</sup>

### **The Need for Active Debris Removal**

Long term forecasting predicts approximately 20 catastrophic collisions during the next 200 years.<sup>6</sup> In December of 2009, DARPA and NASA held the first International Conference on Orbit Debris Removal. More than 50 papers were presented discussing the technology requirements for removal, as well as legal, economic and policy concerns. The need was recognized at the conference for a service vehicle having adequate maneuverability, rendezvous and docking capability, and the ability to make a secure attachment to an arbitrarily rotating object. Projections for the

---

\*"Position Paper on Orbital Debris," (Updated), IAA, September, 2001.

future state of orbital debris show that if all launch activity was stopped now, the debris field would continue to grow, with cascading failures making the space environment essentially unusable by 2100. Projections showing the use of ADR technology demonstrate that if three to five pieces of the most concerning debris objects were removed per year, this environment could be stabilized, and that the removal of ten or more per year would begin the process of mitigating the problem.<sup>4</sup> Figure 2 shows the predicted effect of actively removing objects to mitigate the growth of the debris population. The orbits identified as being of most concern fall into the three regimes<sup>7</sup> shown in Table 1.

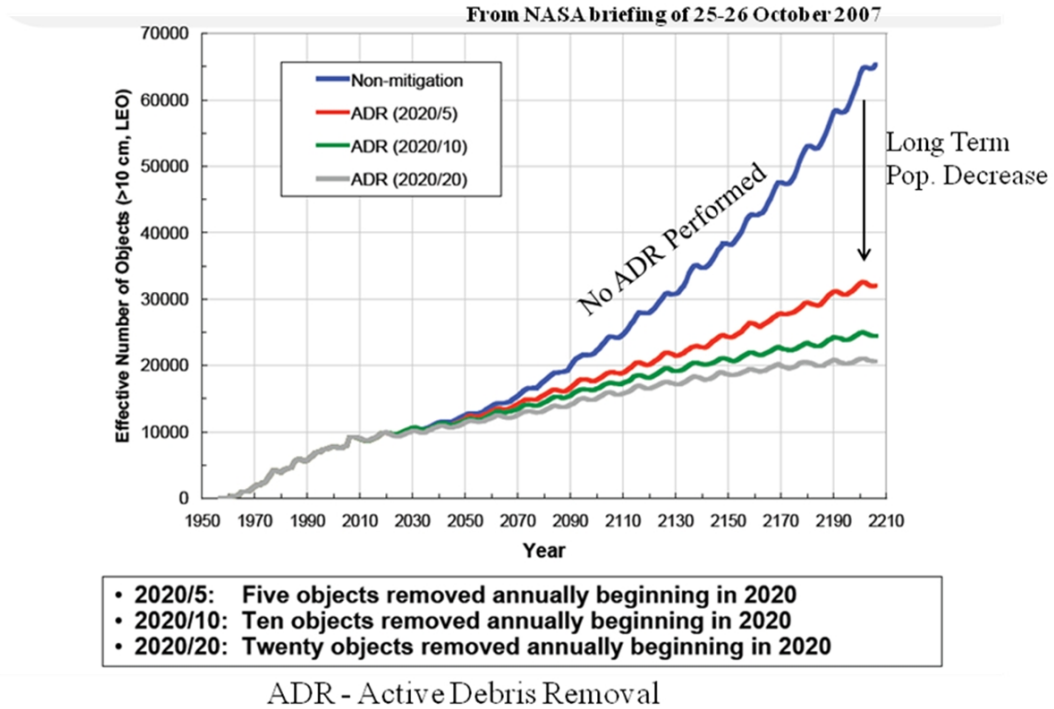


Figure 2. Potential Long Term Benefits of Large Debris Mitigation (From Ref. 1)

Table 1. Most Concerning Orbital Debris Regimes

Orbital Altitude (km)	Inclination	# of Large Objects
1000 ± 100	82° ± 1°	290
800 ± 100	99° ± 1°	140
850 ± 100	71° ± 1°	40

### Approaches to Active Debris Removal

Various approaches to remove debris from space have been proposed, and some seem more technologically feasible than others. Techniques range from attaching tethers, solar sails, or solid rocket motors to debris objects, to active capture via nets followed by removal to other orbits. Of these techniques, one seems particularly feasible and is selected for use in the study presented herein.

*Electro-Dynamic Tethers* The use of Electro-Dynamic Tethers (EDTs) takes advantage of the effect of placing a conductive element in the Earth's magnetic field. The object to be de-orbited is connected via a tether to a de-orbiting element, and both ends have a means of providing electrical contact to the ambient ionospheric plasma. The interaction of the conducting tether moving at orbital speeds induces current flow along the tether, causing a Lorentz force due to the interaction between the tether and the Earth's magnetic field; this causes an acceleration on the object to which the tether is attached. Figure 3 shows a notional EDT system and the resulting force on the spacecraft to which it is attached.

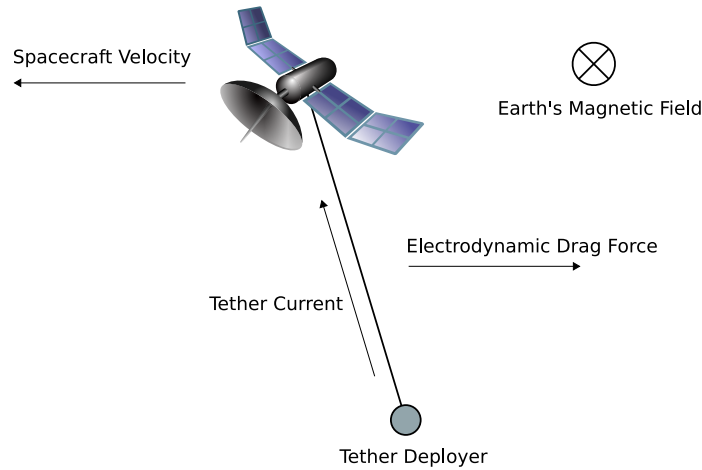


**Figure 3. Electro-Dynamic Tethers Create a Force by Interacting with Plasma in the Earth's Atmosphere**

A tether made of conductive aluminum and massing only 2 to 2.5% of the mass of the object to be de-orbited is sufficient to provide significant deceleration and speed up the de-orbit process.<sup>8</sup> Studies have shown that for high-inclination, low-altitude LEO satellites (e.g., Iridium constellation), the time required for de-orbit from a 780 km altitude orbit can be reduced from 100 years to 1 year. The technology constraints involve potential difficulty in attaching the tether, but this could be done via a harpoon, a hooked net, or an adhesive suction cup. The cross-sectional area and possibility of conjunction collisions with other objects is also increased with the use of the tethers, but less so than with other proposed methods. This approach is the preferred method that our analysis adopts for removal of debris objects from low-Earth orbit.

*Capture and Removal* Capture and removal to a parking/disposal orbit is another promising technique, and various initiatives have been under way to study these scenarios. Essentially, the techniques here involve the capture of an arbitrarily rotating object via robotic arms or other means. The captured object is then moved via a velocity impulse from the ADR vehicle to a new disposal orbit. This technique is not particularly useful in LEO, but is the preferred disposal method in GEO, by which satellites, rocket stages, etc. would be hauled to a higher parking/graveyard orbit, generally referred to as supersynchronous orbit (approximately 300 km above GEO altitude). Research into capture and move techniques has been conducted extensively by European groups, and the results of the Qinetiq ROGER spacecraft scenario have been adopted for this study\* for the purposes of sizing the debris removal spacecraft bus. Additionally, a congressionally mandated satellite ser-

\*"Robotic Geostationary Orbit Restorer (ROGER)," European Space Agency Automation and Robotics Newsletter, November 28, 2006, [http://www.esa.int/TEC/Robotics/SEMTWLKKKSE\\_0.html](http://www.esa.int/TEC/Robotics/SEMTWLKKKSE_0.html)

ving study by the NASA Goddard Space Flight Center (GSFC) has analyzed the GEO capture and move scenario extensively.<sup>9</sup>

*Momentum Exchange Tethers* Momentum exchange tethers are part of another potential solution and involve the tethering of two spacecraft. Generally, a vehicle in a higher orbit will attach a tether to a lower vehicle. The difference in velocity and perturbing accelerations will cause both vehicles to swing along an arc defined by the joining tether. If the lower object is released at the point of greatest retrograde velocity, this will lower its perigee while the apogee will be raised for the higher object. Conceptually, the momentum exchange tether seems promising for ADR activities; however, the theoretical requirements show that a 10 km tether would be required to lower orbit altitude by 100 km. These requirements differ significantly from the requirements for the tethers used in EDT methods and may therefore render momentum exchange tethers infeasible due to the increased collision hazard presented by the large tether size. Another reason why the study presented in this paper does not consider momentum exchange tethers is that the change in the ADR vehicle's orbit is not easily predicted.

*Lasers* Lasers in space raise romantic notions of efficiently vaporizing debris material that could pose a risk to other objects in orbit. The use of lasers for ADR activities is questionable at best, partially due to a requirement to keep a very focused beam pointed at a rapidly and arbitrarily moving target for a long period of time, such that the surface can be ablated enough to induce an acceleration. Moreover, generating adequate levels of power for a space-based laser is beyond our current space power generation capabilities. Additionally, the use of such lasers in space could be problematic with respect to existing international weapons treaties and UN regulations. Also, many of the objects that could be removed may contain unspent propellant that could explode if heated by a laser, thus causing more debris. While lasers may be of some use in removing smaller debris objects, they are not relevant to the study presented herein.

*Surface Material* Surface material or a low density mass in space has also been proposed as a method of debris removal. The basic idea is that a large thin surface material is deployed and objects that strike it experience a change in momentum that slows them down and lowers their orbits. An alternative approach would be to deploy a low density material which would essentially capture or slow material passing through it. The potential exists for such a material to induce a fragmentation event and the resultant deceleration imparted by a material thin enough to avoid this risk is marginal, so these techniques are not considered herein.

*Solar Sails* Solar sails have gained some attention as a possible debris removal technique. Basically, the concept is simple: a reflecting material, which may be very thin, is deployed from an orbiting body and solar photons that strike the material are reflected, imparting an acceleration to the orbiting body. Solar sails are more useful for orbit modifications in which there is no net exchange of energy and are therefore particularly suitable for altering orbital eccentricity. The largest contribution to altitude lowering or de-orbiting actually comes from an increased atmospheric drag rather than the solar/photon effect. But even this is largely unusable at altitudes below 800 km due to the corrosive nature of the ionosphere on the solar sail material.<sup>4</sup> Also, an acceleration that is sufficient to produce a noticeable change in orbit may take months to accumulate. Meanwhile, the cross-sectional area of the debris object is significantly increased by the attached solar sail, thereby increasing the risk of collision or interference with another object.

*Solid Rocket Motors* Solid Rocket Motors (SRMs) attached to a debris object have also been considered. The basic concept would be to launch an ADR vehicle containing multiple small thrust

stages which could be deployed and attached to large debris objects. The problems inherent with this technique include an increased mass at launch due to the required shell and propellant mass of the SRMs and the difficulty in attaching an SRM to an arbitrarily rotating unprepared surface. Even if an SRM could be attached, the module would have to include a complicated attitude determination system so that the motor could be successfully fired at a time when the direction of the resultant change in velocity would serve to lower the orbit of the target debris object.

## APPROACH

We have chosen the EDT as the debris removal system for our analysis, and our goal is to study the capability of spacecraft systems to carry a set of EDTs to multiple debris pieces during the course of a single mission (involving just one launch vehicle). In order to properly study this problem we must next make appropriate assumptions about the dry mass of a sufficiently capable debris removal spacecraft. After that we will be able to apply the aforementioned multi-target rendezvous algorithms to generate near-optimal debris piece rendezvous itineraries.

### Assumptions About Debris Size and ADR Spacecraft Bus

The ROGER spacecraft\* has a launch mass of 3500 kg, of which 2700 kg is propellant. The spacecraft carries 20 throw-nets with a mass of 9 kg each. Subtracting the 2700 kg of propellant and the 180 kg of throw-nets yields a spacecraft dry mass of 620 kg. We then assume that each tether carried by the spacecraft has a mass of 35 kg. This is consistent with 2.5% of the mass of a large rocket stage weighing 1400 kg, which is characteristic of the largest pieces of debris that would be candidates for removal.<sup>8</sup> The dry mass (in kg) of the spacecraft thus becomes a function of the number of debris pieces to be removed, given by

$$m_{dry} = 620 + 35n \quad (1)$$

where  $n$  is the number of debris pieces to be removed. This formula is used to estimate the resulting spacecraft dry mass as a function of  $n$  in the mission design algorithms described in the Results section of this paper.

### Selecting Orbital Debris Removal Targets

The data set used for our analysis is the public Two-Line Element (TLE) catalog distributed by NORAD. The results were derived from MadCAT<sup>10</sup> results for an all-on-all conjunction assessment of 11,970 space objects. The software implementation is a custom application designed specifically to perform conjunction analysis between space objects, but built using a set of Commercial Off-the-Shelf (COTS) software components that can run natively on 32- and 64-bit architectures. To accomplish this assessment, almost 72 million pairs were evaluated over a five day analysis using the public catalog from 11 Feb 2009. These results were obtained from the AGI-prototype MadCAT Machine, a Dell Precision T5400 Intel 2 × 4 Core XEON X5403 3 GHz 64-bit machine with 32 Gigabytes of RAM and 8 processors running Windows XP SP2. This is a high-end computing server that costs around \$3500. It has 10000 RPM hard disk drives for even faster disk access than the standard 7200 RPM drives. For this work, a pairing of objects was declared to have a

---

\*“Robotic Geostationary Orbit Restorer (ROGER),” European Space Agency Automation and Robotics Newsletter, November 28, 2006, [http://www.esa.int/TEC/Robotics/SEMTWLKKKSE\\_0.html](http://www.esa.int/TEC/Robotics/SEMTWLKKKSE_0.html)



conjunction whenever the range between them was less than 5 kilometers (50 km for satellite orbits that come within 200 km of GEO altitude).

The conjunctions predicted by MadCAT were processed to determine how many close approaches each object was involved in during the five day period. A table containing the object number, number of conjunctions, and orbital elements for each object was created. Then the objects were ranked from highest to lowest according to the number of conjunctions they were involved with. Examination of this table revealed that many of the high ranked objects had similar semimajor axis, inclination, and Right Ascension of the Ascending Node (RAAN). This was fortuitous because in order for a multi-object orbital debris removal mission to be achievable with limited propellant (or  $\Delta v$  capability), the objects must be in similar orbits. So the final step in selecting the orbital debris removal targets was to filter the table based on these three orbital elements.

Once the orbital debris removal targets were selected, their orbits were propagated using an SGP-4 propagator over a one year period with a 432 second step size. This step size was chosen to provide more than 10 sample points per orbit yet keep the ephemeris file size manageable. The ephemeris files were then processed by the orbital debris tour trajectory design tool to produce an efficient itinerary.

### Orbital Debris Removal Targets

As previously mentioned, the public catalog of space objects from 11 Feb 2009 was processed by MadCAT for a five day period. Almost 72 million pairs were evaluated and a total of 27724 conjunctions involving 9171 objects were predicted. Object number 28554 was found to have the most conjunctions during the five day period with a total of 83. A histogram that shows the frequency distribution for the number of conjunctions for each object is presented in Figure 4.

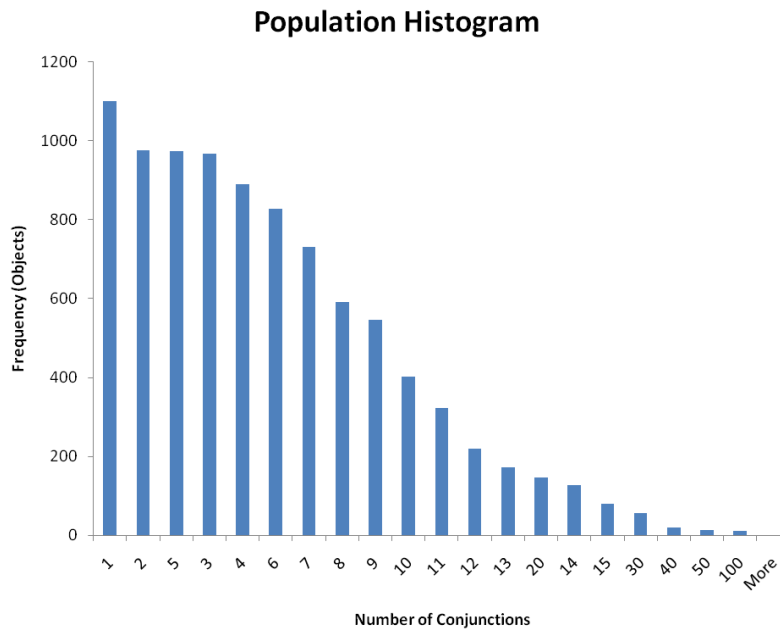


**Figure 4. Population Conjunction Histogram for 11 Feb 2009 through 16 Feb 2009**

A total of 844 objects were involved in 12 or more conjunctions. As previously mentioned, many

of the highest ranking objects had a semimajor axis close to 7200 km and inclination near  $82^\circ$ . By selecting objects with inclination between  $80^\circ$  and  $82^\circ$  and RAAN between  $200^\circ$  and  $360^\circ$ , the 844 objects were pared down to 42, which seemed to be a reasonable number of objects for the trajectory design algorithm to consider. This group of 42 objects contained 9 of 11 objects with 50 or more conjunctions, 8 of 13 objects with 40 to 50 conjunctions, and 7 of 20 objects with 30 to 40 conjunctions, as shown in Table 2.

**Table 2. Conjunction Frequency Distributions for Population and Selected Subset**

Conjunctions	# of Objects in Population	# of Objects in Selected Subset
12	219	1
13	172	0
14	127	3
15	79	1
16–20	147	6
20–30	56	7
30–40	20	7
40–50	13	8
> 50	11	9

### Orbital Debris Removal Tour Itinerary

The orbital debris removal methods considered herein require that the removal spacecraft rendezvous with each piece of orbital debris in turn. Methods for prioritizing and categorizing debris pieces (e.g., according to orbit regime) will produce subsets of the overall debris population, and each piece of debris in the sub-population must be rendezvoused with in turn. Thus the need arises for a means of choosing the order in which the debris pieces are visited that tends to minimize the total  $\Delta v$  required. This will allow the maximum number of debris pieces to be removed per removal spacecraft launch, which in turns help minimize mission costs, minimize the time required to complete a debris removal campaign, and maximize the available payload mass on the removal spacecraft for a given debris removal system. It is worth noting that the number of debris pieces that can be handled by a given debris removal system may be inherently limited and this constraint may take precedence in some cases, but that consideration is beyond the scope of this study.

*Problem Statement and Characterization* The goal is therefore to choose the order for rendezvous for a given set of debris pieces such that the total number of debris pieces that the removal spacecraft is able to visit is maximized. Generally this translates to minimizing the total required  $\Delta v$ . This is similar in character to the famous Traveling Salesman Problem (TSP), in which the order for visiting a set of cities is to be optimized to minimize the total path distance traveled. Strictly optimizing the order in which debris pieces are visited such that the total  $\Delta v$  is formally minimized is daunting since, like the TSP, it is an NP-complete combinatorial optimization problem. This is because the number of permutations of target spacecraft order is practically impossible to exhaustively sample for an interesting number of debris pieces.

*Solution Methodology* The Series Method algorithm offers a computationally efficient means of obtaining a good, if perhaps suboptimal, solution to the problem. The optimality of the Series Method has yet to be characterized and may be addressed in future studies. Subjective assessment of the character of the solutions generated by the Series Method indicates that it is likely at least near-optimal. The Series Method was originally developed for designing interplanetary science

missions to tour near-Earth asteroids (NEAs) and has been used successfully on such problems.<sup>11</sup> In the Series Method, the order for visiting debris pieces is constructed in series, choosing each subsequent debris piece after the first on the basis of minimum  $\Delta v$  to reach the next debris piece, akin to a computer chess program that only looks one move ahead when selecting its next move. Details about the development, structure, and characteristics of the Series Method algorithm can be found in Ref. 11. If a particular debris piece must be visited first, this can be specified; otherwise the algorithm will choose the first target by trying each target as the first when constructing the itineraries and then selecting the choice of first target that serves to maximize the total number of target visits achieved.

To see the computational advantage of the Series Method compared to an exhaustive search, we examine the total number of  $\Delta v$  calculations required. In an exhaustive search all the permutations of target order must be treated and the  $\Delta v$  to travel between targets must be computed for each permutation. The resulting number of  $\Delta v$  calculations for the exhaustive permutation search,  $N_p$ , is therefore given by

$$N_p = (S - 1) \frac{T!}{(T - S)!} \quad (2)$$

where  $S$  is the number of target spacecraft to visit and  $T$  is the total number of available target spacecraft to choose from. Herein we shall consider cases where  $S = T$ , in which case Eq. (2) reduces to

$$N_p = (T - 1) T! \quad (3)$$

The number of  $\Delta v$  calculations performed in the Series Method,  $N_s$ , assuming that each target is tried as the first target in order to find the choice of first target that maximizes the number of targets that can be visited, is

$$N_s = T \sum_{k=1}^{S-1} T - k \quad (4)$$

A comparison of  $N_p$  and  $N_s$  is provided in Table 3 for a range of  $T$  values (target spacecraft population sizes), assuming that  $S = T$ , i.e., all target spacecraft in the population are to be visited. The Series Method is clearly far less computationally expensive than the exhaustive search, allowing target spacecraft populations of interesting sizes (e.g.,  $T > 20$ ) to be handled readily on standard workstation computers. By contrast, treating such population sizes with an exhaustive search would require extremely large supercomputers. However, the number of calculations required for exhaustive search solutions for small target populations ( $T < 7$ ) is tractable, enabling future studies that will characterize the optimality of the Series Method statistically.

Other numerical methods for solving this orbital version of the TSP might also be pursued, such as simulated annealing and/or genetic algorithms. Such algorithms are known to be capable of providing practical optimal or near-optimal solutions to TSP type problems and may be explored in future work. Their efficacy, computational expense, complexity, and robustness would be compared to those qualities of the Series Method.

**Table 3. Number of  $\Delta V$  Calculations Required by Exhaustive Search and Series Method**

$T$	$N_p$	$N_s$
3	12	9
4	72	24
5	480	50
7	30,240	147
10	$3.265920 \times 10^7$	450
20	$4.622514 \times 10^{19}$	3,800
30	$7.692333 \times 10^{33}$	13,050
40	$3.182070 \times 10^{49}$	31,200
100	$9.239295 \times 10^{159}$	495,000

## RESULTS

The set of 42 debris pieces defined previously was subjected to multi-target rendezvous trajectory analysis via the Series Method algorithm just described. This yielded an array of required total spacecraft launch masses as a function of the number of debris pieces visited and the specific impulse of the debris removal spacecraft's thruster. These required launch masses were then compared to the published capabilities of existing launch vehicles to assess the feasibility of removing various quantities of debris.

### Orbital Debris Removal Tour Itinerary Results

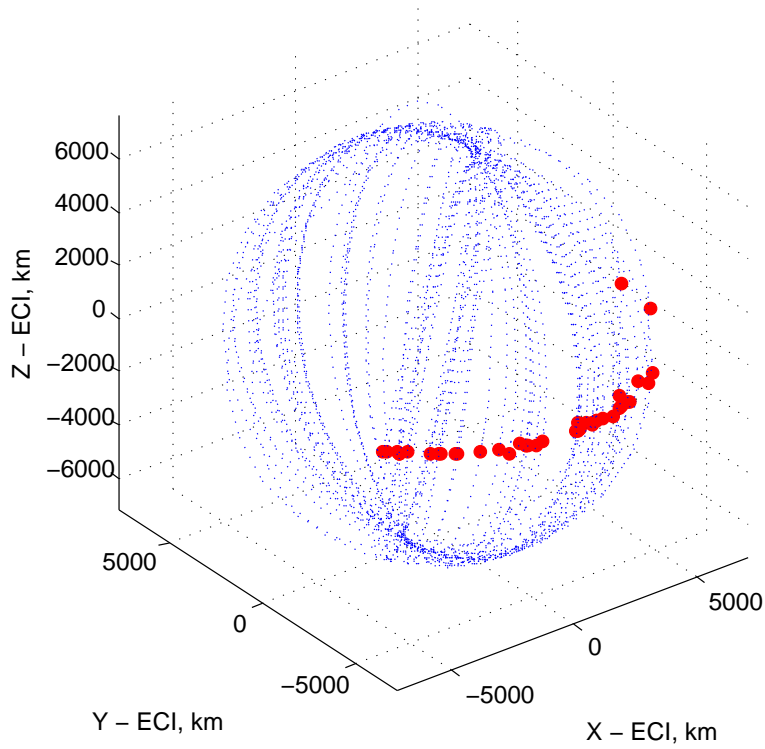
The orbits of the 42 debris pieces were propagated using two-body dynamics and making the deliberate approximation of treating the two-line elements as osculating elements just to provide a visual impression of the debris piece orbits under consideration. A plot showing these orbits is presented in Figure 5.

It is clear that these orbits mostly occupy different planes. This is because while they all have similar inclination angles (between  $80.5^\circ$  and  $82^\circ$ ), they all have different right ascensions of the ascending node. The differences between their orbit planes will clearly have a strong impact on the  $\Delta v$  required to travel between them. It would be fortuitous if large groups of debris pieces tended to reside in nearly similar orbit planes, but natural orbit perturbations tend to preclude this, particularly in LEO.

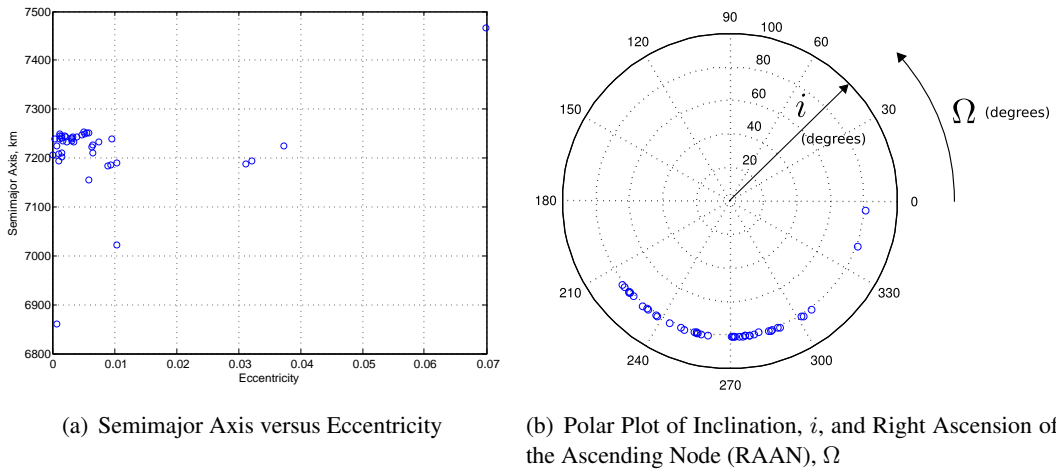
Figure 6(a) presents the relationship between the semimajor axes and eccentricities of the debris piece orbits. All of the debris pieces have similar semimajor axes and eccentricities, except for a few with slightly higher, but still small, eccentricities. Most of the orbits are not far from circular and have an altitude near 845 km.

Figure 6(b) makes clear the nature of the debris piece orbit planes suggested by Figure 5; all the debris pieces have an inclination angle near  $81^\circ$  but have different right ascensions, clustered mostly between  $210^\circ$  and  $310^\circ$ . While the natural nodal drift caused by  $J_2$  might be exploited in the design of multi-target rendezvous trajectories, we did not have the resources to pursue that idea in this study and have relegated it to future work.

Table 4 presents the launch mass capabilities of various launch vehicles in the Delta series of rockets to a circular orbit of 845 km altitude at  $81.2^\circ$  inclination, as this corresponds to the first debris piece in the itinerary identified by applying the Series Method. These launch vehicle performance



**Figure 5. Orbits of the 42 Debris Pieces**



**Figure 6. Orbit Size, Shape, and Orientation for the 42 Debris Pieces**

data are approximate and were derived from the Kennedy Space Center (KSC) NASA Launch Services Programs Launch Vehicle Performance Web Site\*. Table 4 includes several variants of the

\*<http://elvperf.ksc.nasa.gov/elvMap/>. Note that while the Delta launch vehicles were available at the time when our analysis was performed, they are not part of NASA's current launch contract (NLS-II).

**Table 4. Derived Approximate Launch Vehicle Performance Parameters**

Launch Vehicle	Launch Mass (kg) to 845 km, 81.2°
Delta II (2320-9.5)	1523
Delta II (2320-10)	1598
Delta II (2420-10)	1847
Delta II (2420-9.5)	1940
Delta II (2920-10L)	2809
Delta II (2920-10)	2875
Delta II (2920-9.5)	2972
Delta IV (4040-12)	7149
Delta IV (4240-12)	9647
Delta IV (4450-14)	10772
Delta IV (4050H-19)	20963

Delta II and Delta IV launch vehicles.

The Series Method algorithm was executed on the 42 debris pieces using Lambert targeting to compute the rendezvous trajectories between debris pieces. The algorithm was set to construct an itinerary for visiting 32 of the debris pieces and to try each of the 42 pieces as the first target, selecting the choice of first target that served to minimize the total  $\Delta v$ . The total  $\Delta v$  computed for the rendezvous sequence for 32 target objects was approximately 12 km/s. This is substantial and was driven, as predicted, by the plane changes required to travel between the debris pieces. The total time required for the rendezvous sequence for 32 debris pieces was 260 days and includes some stay time at each debris piece for terminal rendezvous, proximity operations, capture, tether attachment, release, and departure. For the current study we have estimated the total  $\Delta v$  for these activities to be 20 m/s and this will be refined in future work.

The trajectory design results were then subjected to a post-processing step in which the total required launch mass was computed as a function of the spacecraft dry mass, which is a function of the number of debris pieces to visit as specified in Eq. (1), and the spacecraft thruster specific impulse. Six representative values of specific impulse were selected: 200, 300, 450, 1600, 2200, and 3000 seconds. The values of 200 and 300 seconds serve to bound the typical performance of high-thrust conventional hypergolic propulsion systems while 450 seconds represents the upper limit for conventional propulsion (achieved using cryogenic propellant).

The values of 1600, 2200, and 3000 seconds serve to represent low, medium, and high performance low-thrust propulsion systems, respectively. While no low-thrust trajectory design was actually performed in this study, the total  $\Delta v$  requirements will generally be similar\* to what we computed for the impulsive maneuver ballistic trajectories and so utilizing the low-thrust propulsion system performance parameters in this study sheds light on how low-thrust technology might aid the debris removal effort. However, it is worth noting that the required flight times for the low-thrust trajectories would tend to be substantially longer than what we computed here for the high-thrust trajectories.

Table 5 presents the post-processing results in terms of required launch mass to rendezvous with each of 5 to 32 debris pieces using spacecraft thruster specific impulses ranging from 200 to 3000

---

\*Total  $\Delta v$  for low-thrust trajectories tends to be somewhat higher than for ballistic trajectories due to kinematic inefficiencies.

**Table 5. Required Spacecraft Launch Mass (kg) as a Function of Dry Mass and Thruster Specific Impulse for the Series Method Itinerary Using Lambert Targeting**

# of Targets	Dry Mass (kg)	Thruster Specific Impulse (seconds)					
		200	300	450	1600	2200	3000
5	795	1312	1110	993	846	832	822
6	830	1428	1191	1056	888	871	860
7	865	3100	2025	1525	1014	971	941
8	900	3613	2273	1669	1070	1021	987
9	935	4090	2501	1801	1124	1069	1031
10	970	5718	3165	2134	1210	1139	1091
11	1005	5987	3302	2221	1256	1182	1131
12	1040	8997	4382	2713	1361	1265	1200
13	1075	16991	6770	3666	1517	1381	1292
14	1110	22529	8259	4230	1617	1459	1356
15	1145	30699	10257	4938	1727	1544	1425
16	1180	36645	11658	5433	1813	1612	1483
17	1215	41640	12819	5844	1889	1675	1537
18	1250	52920	15184	6605	1996	1757	1604
19	1285	61099	16865	7149	2082	1825	1662
20	1320	77829	19996	8081	2197	1912	1732
21	1355	88266	21937	8671	2283	1980	1790
22	1390	92590	22841	8984	2349	2036	1839
23	1425	97689	23869	9328	2417	2092	1888
24	1460	108947	25877	9925	2502	2160	1946
25	1495	146384	31759	11467	2651	2267	2029
26	1530	186546	37620	12937	2789	2367	2107
27	1565	245944	45575	14813	2944	2478	2192
28	1600	471343	70837	20023	3256	2682	2337
29	1635	528121	76971	21316	3366	2764	2403
30	1670	564153	81003	22211	3457	2835	2462
31	1705	632860	88060	23646	3572	2919	2529
32	1740	752661	99521	25830	3715	3021	2607

seconds. Table 5 is color-coded to indicate which combinations of number of debris pieces and thruster specific impulse can be handled by particular groups of launch vehicles. Some solutions can be handled by the Delta II rockets (colored green in the table), some only by the Delta IV rockets (colored yellow in the table), and some solutions are not possible even with the largest rocket, the Delta IV Heavy (colored red in the table). As described previously, the dry mass is a direct function of the number of objects to be visited as this affects the number of EDTs required for a given mission.

The results shown in Table 5 are presented in a different way in Table 6, showing how many debris pieces can be de-orbited *in less than a year* via EDTs for each combination of launch vehicle and thruster. These results are fairly promising; even the least capable launch vehicle and thruster are capable of de-orbiting 6 pieces of debris. The smallest of the Delta IV series of launch vehicles is capable of de-orbiting 11 pieces of debris even with the least capable thruster. The largest (and most expensive) launch vehicle, the Delta IV Heavy, is capable of de-orbiting 20 pieces of debris, with

**Table 6. Number of Debris Pieces Reached as a Function of Launch Vehicle and Debris Removal Spacecraft Thruster Specific Impulse - Lambert Targeting Rendezvous Method**

Launch Vehicle	Thruster Specific Impulse (seconds)					
	200	300	450	1600	2200	3000
Delta II (2320-9.5)	6	6	6	13	14	16
Delta II (2320-10)	6	6	7	13	15	17
Delta II (2420-10)	6	6	9	16	19	22
Delta II (2420-9.5)	6	6	9	17	20	23
Delta II (2920-10L)	6	9	12	26	29	35
Delta II (2920-10)	6	9	12	26	30	35
Delta II (2920-9.5)	6	9	12	27	31	36
Delta IV (4040-12)	11	13	18	40	42	42
Delta IV (4240-12)	12	14	23	42	42	42
Delta IV (4450-14)	12	15	24	42	42	42
Delta IV (4050H-19)	13	20	28	42	42	42

the spacecraft using a moderately capable conventional thruster. Note that increasing the specific impulse, as would be the case if low-thrust spacecraft propulsion was used, shows that it might be possible to de-orbit all 42 pieces of debris when used with one of the Delta IV launch vehicles (not necessarily the Delta IV Heavy). Detailed low-thrust trajectory design needs to be performed to verify this result and determine how much mission time would be required, but the preliminary results obtained here are promising.

The Series Method analysis was repeated using a co-elliptic rendezvous strategy in lieu of Lambert targeting to travel between the debris pieces. The co-elliptic rendezvous method uses Gauss' form of the Lagrange Planetary Equations to compute the maneuvers required to match orbit plane, apse lines, and eccentricity with the target object and achieve a semimajor axis slightly below or above. Natural relative drift due to the difference in orbit altitude then brings the objects close together, at which point terminal rendezvous can commence. The  $\Delta v$  required for the rendezvous and capture is then computed. The total  $\Delta v$  computed using this method is very similar to that computed using the Lambert targeting, except that the total  $\Delta v$  in the co-elliptic method includes the rendezvous, proximity operations, and capture  $\Delta v$ .

Table 7 presents the number of debris pieces that can be reached as a function of launch vehicle and debris removal spacecraft thruster, similar to Table 6 except that here the co-elliptic rendezvous method is being utilized and the rendezvous, proximity operations, and capture  $\Delta v$  is included. Overall, the performance is nearly the same as for the Lambert targeting case, providing a valuable cross-check and verification.

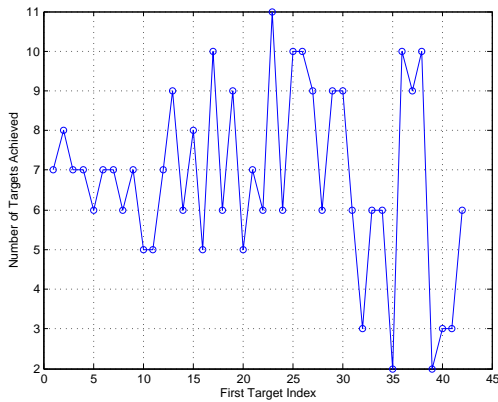
The impact of the choice of first target is shown in Figures 7(a) and 7(b). Figure 7(a) shows the number of target visits achieved with a particular spacecraft and launch vehicle configuration, with a goal of achieving 11 debris pieces. Only one choice of first target allows 11 targets to be reached. Several poor choices of first target allow only 2 or 3 targets to be reached, while most choices of first target allow only 5 to 8 targets to be reached. A similar situation is shown in Figure 7(b) in which the goal was to reach 42 objects.

The nature of the Series Method solutions (with best choice of first target) is shown in Figures 8(a) and 8(b). The distribution of right ascensions of ascending nodes for the target debris pieces produces the wide variation in their orbit planes, and this tends to drive the total  $\Delta v$  required to travel

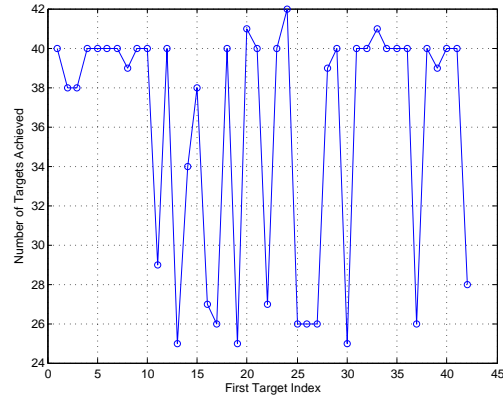


**Table 7. Number of Debris Pieces Reached as a Function of Launch Vehicle and Debris Removal Spacecraft Thruster Specific Impulse - Co-Elliptic Rendezvous Method**

Launch Vehicle	Thruster Specific Impulse (seconds)					
	200	300	450	1600	2200	3000
Delta II (2320-9.5)	5	6	8	15	16	17
Delta II (2320-10)	5	7	9	15	17	19
Delta II (2420-10)	6	8	10	19	21	23
Delta II (2420-9.5)	8	10	13	25	30	35
Delta II (2920-10L)	8	11	13	25	30	35
Delta II (2920-10)	8	11	13	26	31	35
Delta II (2920-9.5)	8	11	14	27	32	36
Delta IV (4040-12)	12	15	20	40	42	42
Delta IV (4240-12)	13	17	22	42	42	42
Delta IV (4450-14)	13	17	23	42	42	42
Delta IV (4050H-19)	16	20	27	42	42	42



(a) 11 Target Rendezvous Sequence



(b) 42 Target Rendezvous Sequence

**Figure 7. Variation in the Number of Debris Pieces Visited as a Function of the Choice of First Target**

between them. The Series Method naturally finds an efficient ordering of the objects in terms of right ascension of the ascending node, and this is made evident in Figures 8(a) and 8(b). The evolution of the spacecraft fuel mass for these two cases is shown in Figures 9(a) and 9(b).

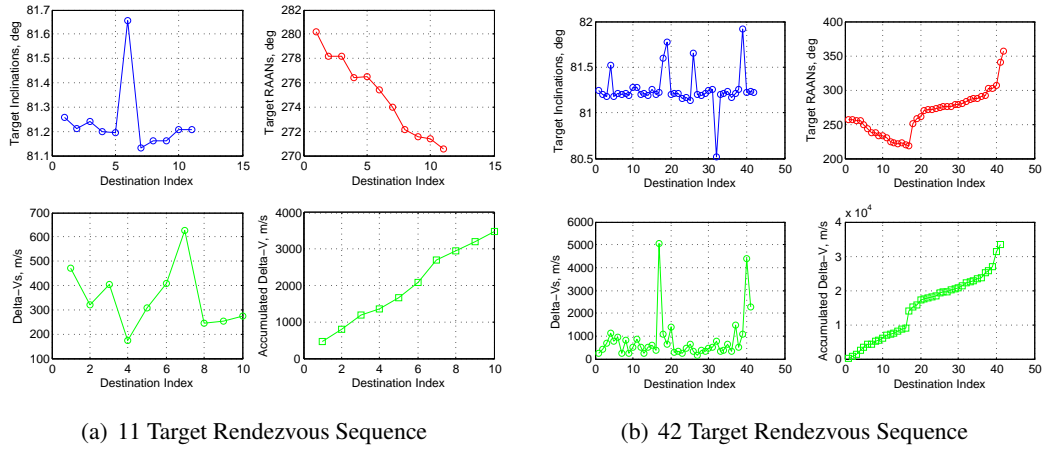


**Figure 8. Ordering of Target Debris Piece Inclination and RAAN Angles Produced by The Series Method, with Corresponding  $\Delta v$  Evolution**

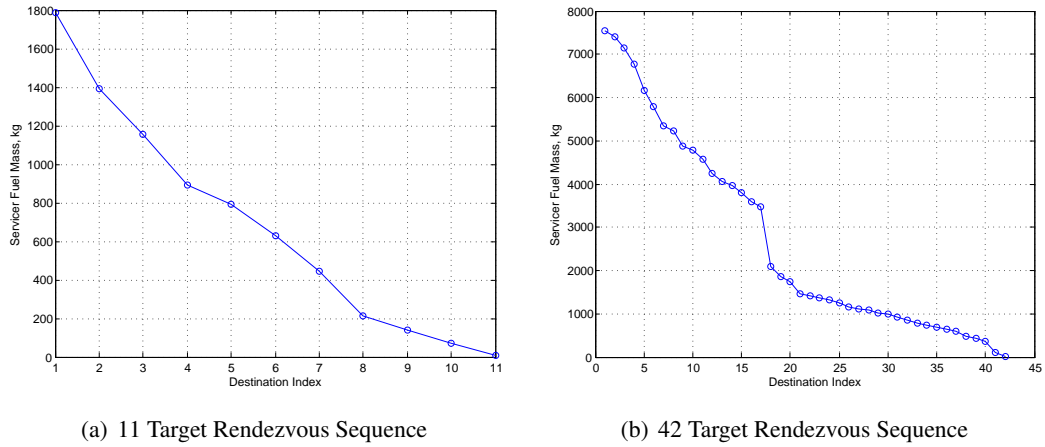


**Figure 9. Spacecraft Fuel Mass Evolution**

## CONCLUSIONS

Preliminary mission design results indicate that removing 5 to 10 pieces of orbital debris annually should be quite feasible using existing launch vehicle and propulsion technology. Removing > 20 pieces of debris within one year using a single spacecraft is also a feasible proposition, particularly if high specific impulse propulsion technology is utilized in combination with heavy lift launch vehicles. However, these results are quite dependent on the requisite assumptions about spacecraft dry mass. Furthermore, additional analysis is required to fully treat the problem of autonomous rendezvous, proximity operations, and capture of non-cooperative objects and the required absolute and relative navigation techniques and technologies. Nevertheless, the basic physics and orbital mechanics of the problem currently appear to support the conclusion that orbital debris removal is feasible and affordable with current launch vehicle and spacecraft propulsion technologies.

## Future Work

The authors realize that this study is conceptual and only addresses some of the fundamental problems associated with deploying ADR technology. Specifically, assumptions were made about the ability to attach a de-orbiting electrodynamic tether to an orbital debris object. The focus of this study was to determine efficient multi-target trajectories that would allow a single spacecraft to remove as many pieces of debris as possible during a single mission. Since the criteria for target selection involves high conjunctions, future work may analyze the possible conjunctions of the ADR vehicle with other orbiting objects to address safety concerns. The assumptions used here also propagate orbital elements from the publicly available TLEs over long periods of time. This is not a perfectly valid assumption as TLEs are meant only for short term propagation. In future work, the calculation of the state of the next object will take into account the evolved TLEs at the given epoch. Additionally, the best solution for removing debris in GEO would seem to involve a capture and move of the target object, and the calculation of the next target would necessarily be from the graveyard orbit to the next object. The Series Method is fully capable of supporting this scenario. Some consideration was also given to the large propellant requirements for attempts to remove more than 10 debris objects with a single ADR vehicle, and to the possibility of utilizing an on-orbit propellant depot that the ADR vehicle could use to replenish its propellant tanks as needed. However, the requirements to maintain the propellant depot would seem, at first consideration, to require a large use of propellant to avoid drift, and thus seem inadequate for the missions considered here. Also, the propellant required for the ADR spacecraft to travel to and from the depot might reduce or eliminate the advantages offered by the presence of the depot. Other studies of this concept confirm these suspicions.<sup>9</sup> Finally, the Series Method may be applied along with optimal low-thrust trajectory design algorithms to properly evaluate the performance of low-thrust spacecraft for orbital debris removal missions.

## ACKNOWLEDGMENT

The authors would like to note that the research described in this paper was performed solely because of the authors' collective interest in the problem and is not part of a funded project.

## REFERENCES

- [1] Payne, T. and Morris, R., "The Space Surveillance Network (SSN) and Orbital Debris," 33<sup>rd</sup> Annual AAS Guidance and Control Conference, AAS Paper Number 10-012, February 6–10 2010. Breckenridge, Colorado.

- [2] Johnson, N. L., "Orbital Debris: The Growing Threat to Space Operations," 33<sup>rd</sup> Annual AAS Guidance and Control Conference, AAS Paper Number 10-011, February 6–10 2010. Breckenridge, Colorado.
- [3] Stansbery, G., Liou, J.C., Mulrooney, M., and Horstman, M., "Current and Near-term Future Measurements of the Orbital Debris Environment at NASA," 33<sup>rd</sup> Annual AAS Guidance and Control Conference, AAS Paper Number 10-013, February 6–10 2010. Breckenridge, Colorado.
- [4] Matney, M., "An Overview of NASA's Orbital Debris Environment Model," 33<sup>rd</sup> Annual AAS Guidance and Control Conference, AAS Paper Number 10-014, February 6–10 2010. Breckenridge, Colorado.
- [5] Gavin, R. T., "NASA's Orbital Debris Conjunction Assessment and Collision Avoidance Strategy," 33<sup>rd</sup> Annual AAS Guidance and Control Conference, AAS Paper Number 10-015, February 6–10 2010. Breckenridge, Colorado.
- [6] Kessler, D. J., Johnson, N. L., Liou, J. C., and Matney, M., "The Kessler Syndrome: Implications to Future Space Operations," 33<sup>rd</sup> Annual AAS Guidance and Control Conference, AAS Paper Number 10-016, February 6–10 2010. Breckenridge, Colorado.
- [7] Klinkrad, H. and Johnson, N. L., "Sustainable Use of Space Through Orbital Debris Control," 33<sup>rd</sup> Annual AAS Guidance and Control Conference, AAS Paper Number 10-017, February 6–10 2010. Breckenridge, Colorado.
- [8] Pearson, J., "The ElectroDynamic Debris Eliminator (EDDE): Removing Debris in Space," *Orbital Debris Quarterly News*, Vol. 14, January 2010.
- [9] Barbee, B. W., Carpenter, J. R., Heatwole, S., Markley, F. L., Moreau, M., Naasz, B. J., and Van Eepoel, J., "Guidance and Navigation for Rendezvous and Proximity Operations with a Non-Cooperative Spacecraft at Geosynchronous Orbit," George H. Born Symposium, May 2010. Boulder, Colorado.
- [10] Coppola, V. T., Dupont, S., Ring, K., and Stoner, F., "Assessing Satellite Conjunctions for the Entire Space Catalog Using COTS Multi-core Processor Hardware," AAS/AIAA Astrodynamics Specialist Conference, AAS Paper Number 09-374, August 9–13 2009. Pittsburgh, Pennsylvania.
- [11] Barbee, B. W., Davis, G. W., and Hur-Diaz, S., "Spacecraft Trajectory Design for Tours of Multiple Small Bodies," *Advances in the Astronautical Sciences*, Vol. 135, 2009, pp. 2169–2188. also AAS/AIAA Paper AAS 09-443, Astrodynamics Specialists Conference, Aug. 2009.